Laser Ion-Acceleration Scaling Laws Seen in Multiparametric Particle-in-Cell Simulations

T. Esirkepov,* M. Yamagiwa, and T. Tajima
Kansai Photon Science Institute, JAEA, Kizu, Kyoto, 619-0215 Japan
(Received 24 October 2005; published 14 March 2006)

The ion acceleration driven by a laser pulse at intensity $I = 10^{20}$–10^{22} W/cm$^2 \times (\mu\text{m}/\lambda)^2$ from a double layer target is investigated with multiparametric particle-in-cell simulations. For targets with a wide range of thickness l and density n_e, at a given intensity, the highest ion energy gain occurs at certain *electron areal density* of the target $\sigma = n_e l$, which is proportional to the square root of intensity. In the case of thin targets and optimal laser pulse duration, the ion maximum energy scales as the square root of the laser pulse power. When the radiation pressure of the laser field becomes dominant, the ion maximum energy becomes proportional to the laser pulse energy.

DOI: 10.1103/PhysRevLett.96.105001 PACS numbers: 52.38.Kd, 29.25.−t, 41.75.Lx, 52.65.Rr

Laser-driven ion acceleration can be of benefit for many applications, e.g., hadron therapy in oncology [1], fast ignition of thermonuclear fusion by protons [2], production of sources for positron emitting tomography [3], conversion of radioactive waste [4], etc. The radiation pressure dominant (RPD) regime of laser ion acceleration [5] can be a basis for a laser-driven heavy ion collider and proton dump facility for neutrino oscillation studies [6]. All these applications can become possible owing to invention of high-intensity lasers [7], which now are capable to produce pulses with intensity 10^{20}–10^{22} W/cm^2.

Irradiation of solid targets by lasers with power from terawatt to petawatt (PW) and intensity up to 10^{21} W/cm^2 resulted in generation of proton beams with maximum energy $\mathcal{E}_{\max}$ from 1 up to about 60 MeV [8]. Typical proton beam has picosecond duration and is emitted in quasilaminar fashion [9]; it can have very low transverse emittance [10]. Experiments indicate that the proton energy increases with the laser intensity, and it depends also on the target (foil) thickness and the target composition. It turns out that for a given laser intensity there is an optimal target thickness, at which the proton energy is maximum [11]. Thus, the important question is what the ion maximum achievable energy is at a given intensity and how it scales with increasing intensity.

In this Letter, we investigate the scaling laws of the ion acceleration driven by a laser pulse at intensity $I = 10^{20}$–10^{22} (W/cm^2)$(\mu\text{m}/\lambda)^2$ from a *double layer target* with *multiparametric* two-dimensional particle-in-cell (PIC) simulations. The double layer target was suggested in Ref. [1] for a high-quality ion beam generation suitable for hadron therapy. In publications, one can find several regimes of laser-driven multi-MeV ion acceleration from foil targets. Ions can be accelerated by a *varying* electrostatic potential of the electron cloud expanding into vacuum, as shown in Ref. [12]. In the case of thin foils, when the laser pulse quickly sweeps a significant part of the electrons away, the ion acceleration can occur in a *quasisteady* potential [1,13]. Below, we show that, according to our simulations, in the case of thin targets and optimal laser pulse duration, the ion maximum energy scales as the square root of the laser pulse power, as suggested in Ref. [13]. At higher intensity, when the radiation pressure of the laser field becomes dominant, the plasma is accelerated so that almost all the energy of the laser pulse is transformed into ion energy [5].

We study the idealized model, where the ''clean'' Gaussian p-polarized laser pulse is incident at a right angle on a thin slab of ideal collisionless plasma. We note that, in experiments cited here, laser pulses have low-intensity parts, such as prepulse and amplified spontaneous emission (ASE), which can change the structure of the solid target before the main part of the laser pulse arrives; e.g., a preplasma can be formed. This effect is discussed in Refs. [14,15]. The approximation of collisionless plasma can be satisfactory when a femtosecond laser at intensity $\gtrsim 10^{20}$ W/cm^2 interacts with the plasma slab, which is a few laser wavelengths thick, even at the solid density of plasma. The laser pulse is characterized by the wavelength λ, the length L_p (FWHM), focal spot diameter D (FWHM), and the dimensionless amplitude a, corresponding to intensity $I = a^2 I_1$, $I_1 = 1.368 \times 10^{18}$ W/cm$^2 \times (\mu\text{m}/\lambda)^2$. The target consists of two layers; the first layer is fully stripped aluminum, and the second layer is a proton coating. The first and second layers of the target are described, respectively, by the electron density n_e and n_{e2}, the thickness l and l_2, and the transverse (perpendicular to the laser pulse direction) size w and w_2.

We carried out multiparametric simulations using a technique described in Ref. [15]. In this technique, a series of N tasks with different sets of laser and target parameters is performed simultaneously on the N processors of a multiprocessor supercomputer, using the massively parallel and fully vectorized code REMP, based on the PIC method and the ''density decomposition'' scheme [16]. We analyze the dependence of the interaction outcomes such as reflection, transmission and absorption coefficients, energy spectra of ions and electrons, beam emittance, the acceleration time and length, etc., on parameters of the laser pulse and the target: laser pulse intensity I, focal spot size D and duration L_p/c, target density n_e, and

thickness l. In the simulations, the laser pulse initially propagates along the x axis in the simulation box with $x \times y$ size $251\lambda \times 136\lambda$; the transverse size of the target first layer is fixed: $w = 80\lambda$; for the second layer it is $w_2 = D/2$; the second layer is 0.06λ thick; its density is such that the number of ions in the first layer in the longitudinal direction is $\sim 10^3$ times greater than the corresponding number of protons. The number of protons varies from 10^7 to 10^9 in simulations shown in Fig. 1 and from 10^8 to 10^{10}—in Fig. 2. At chosen conditions, the proton layer is accelerated as a whole. The resulting proton beam transverse emittance is less than 0.1π mm mrad. Simulations were performed on HP Alpha Server at JAERI–Kansai and SGI Altix at JAEA–Tokai. In each processor, the grid consists of 4016×2176 cells and a number of quasiparticles is 1.9×10^7, amounting to 6.3×10^9 of cells and 1.4×10^{10} of quasiparticles in total.

Figure 1 shows how the proton maximum energy depends on the target thickness and density and the laser intensity for fixed laser length $L_p = 10\lambda$ and focal spot size $D = 10\lambda$. The proton energy was taken at the time when the (kinematic) acceleration of the center of inertia of protons dropped to 3% from maximum; the corresponding acceleration length is approximately equal to the laser focal spot size. Figures 1(a)–1(e) represent the results of 720 separate computational tasks performed simultaneously in one run on a 720-processor supercomputer; each point with coordinates (l, n_e) at fixed intensity I corresponds to a particular one-processor task. The target thickness changes in the range $l/\lambda = 0.1$–5 (12 samples); the target density varies from $n_e = n_{cr}$ to $100n_{cr}$ (12 samples), where $n_{cr} = \pi/(r_e\lambda^2)$ is the critical density and $r_e = e^2/m_e c^2$ is the classical electron radius. The intensity varies from $I = 10^{20}$ to $10^{22}\,\mathrm{W/cm^2} \times (\mu\mathrm{m}/\lambda)^2$ (5 samples). A plasma slab with comparatively low density and large thickness can be considered as a model of the target modified by low-intensity parts of the laser pulse (prepulse and/or ASE).

In Fig. 1, the ion energy curves are nearly parallel to the contours of the *electron areal density* $\sigma = n_e l$. Thus, the energy dependence on two parameters l and n_e degenerates to a dependence on only one parameter σ, which is rather surprising if we inspect different results corresponding to the same σ. At small thickness l and large density n_e, the laser pulse sweeps away a substantial part of electrons, and the induced strong Coulomb potential of the first layer accelerates protons, in accordance with Refs. [1,13]. At large thickness and small density, the laser pulse generates a strong quasistatic magnetic field whose pressure causes charge separation, which accelerates protons near the plasma-vacuum interface, similarly to the mechanism suggested in Refs. [15,17].

The maximum of the ion energy gain corresponds to a certain optimal electron areal density σ_{opt}. For decreasing $\sigma < \sigma_{opt}$, more and more laser pulse energy is transmitted through the plasma slab. For increasing $\sigma > \sigma_{opt}$, the laser pulse reflection becomes more and more efficient. At $\sigma = \sigma_{opt}$, the absorption of the laser energy turns out to be optimal for ion acceleration. The proton energy spread is below 5% for $\sigma \leq \sigma_{opt}$; it increases for $\sigma > \sigma_{opt}$. The optimal electron areal density almost linearly depends on the square root of the laser intensity $\sigma_{opt}/n_{cr}\lambda \approx 3 + 0.4(I/I_1)^{1/2}$. This is similar to the criteria of relativistic transparency of a thin foil [18]. In a rough interpretation, ions are accelerated by the electrostatic field of the charge separation caused by the laser pulse. The electrons, if their number is large, can form the electric current which is sufficient to reflect the laser pulse. However, this current cannot be greater than the limiting electric current $\approx -en_e c$. Therefore, at increasing laser intensity, the reflection becomes less and less efficient, plasma becomes more and more transparent, and at some point all the electrons are involved into the interaction. With even greater laser intensity, an even larger number of electrons could be disturbed, providing stronger charge separation; therefore, a smaller number of electrons will not be optimal. Thus, for every value of the laser intensity, there is a certain optimal limiting electric current. Since this effect is mainly one-dimensional, the limiting current is defined by the electron areal density of the slab, as in Ref. [18].

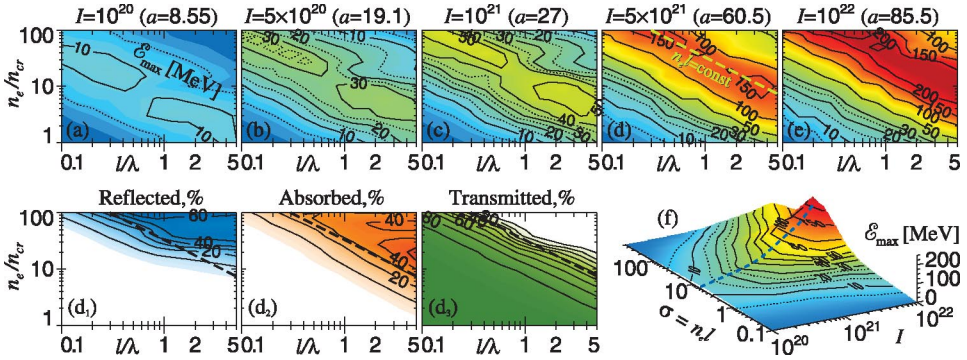

FIG. 1 (color). Proton maximum energy (contours) vs target thickness and density (log-log scale) for different laser intensities (a)–(e), for $L_p = 10\lambda$, $D = 10\lambda$. The laser pulse (d_1) reflection, (d_2) absorption, and (d_3) transmission coefficients related to frame (d). The dashed line in (d), (d_{1-3}) is for the best $n_e l$, corresponding to maximum energy gain. (f) Proton maximum energy vs laser intensity and target electron areal density $\sigma = n_e l$ (log-log scale). The dashed line is for optimal $\sigma_{opt} \propto I^{1/2}$. Intensity unit $\mathrm{W/cm^2} \times (\mu\mathrm{m}/\lambda)^2$.

Figure 1(f) shows the dependence of the ion energy gain on the laser intensity I and the electron areal density σ. Varying the σ, one can find the minimum intensity which gives the desired energy gain. Varying parameters l, n_e. and I simultaneously, one can obtain practically arbitrary scaling, e.g., $\mathcal{E}_{\max} \propto I^{\chi}$, $\chi \geq 1/2$.

Figure 2 shows the proton maximum energy vs the laser length and the target thickness for different laser intensities and focal spots at fixed plasma density $n_e = 100 n_{\rm cr}$. As above, the proton energy corresponds to the time when the acceleration damped to 3% from maximum. The laser pulse length is chosen in the range $L_p/\lambda = 10$–60 (6 samples), the target thickness is $l/\lambda = 0.125$–5 (8 samples), the laser intensity samples are the same as above, and the laser focal spot diameter choices are $D/\lambda = 10, 25, 50$. We see that, for the given range of parameters, the energy gain increases with decreasing target thickness and increasing laser pulse length. From the results of this simulation, the proton energy spread can be approximated by $\Delta\mathcal{E}/\mathcal{E}_{\max} \approx 70 l/(L_p a)$; it is almost independent of the focal spot diameter. Columns (b) and (c) in Fig. 2 indicate that energy in the range 100–200 MeV is achievable with a clean petawatt laser with subpicosecond duration when the solid density target is sufficiently thin, as was found in Ref. [19].

At intensity of the order of 5×10^{21} W/cm^2 $\times$ $(\mu{\rm m}/\lambda)^2$, the new regime of acceleration comes into play, when the energy gain rapidly increases with the laser pulse length, and, for the optimal pair of laser duration and target thickness, relativistic protons can be obtained. This is the *radiation pressure dominant* regime of the ion acceleration, described in Ref. [5] for much higher intensity. In this case, the laser radiation pressure dominates in the interaction, and the effective cross section of the process (analog of the Thomson cross section) becomes $2/n_e l$ [5]. As shown in Fig. 2, the energy gain decreases if the laser duration is greater than the optimum. This is because we use Gaussian laser pulses: a long, relatively weak, front of the pulse has time to deteriorate the target. As indicated in Ref. [5], in the ideal case of the RPD regime, the energy gain is proportional to the laser pulse duration.

Figures 3 and 4 are compiled from the results presented above. In Fig. 3, the proton maximum energy $\mathcal{E}_{\max}$ is drawn for every instance of the laser pulse energy $\mathcal{E}_{\rm L}$ in the case $l = \lambda$, $n_e = 100 n_{\rm cr}$. Points become arranged along 3 lines corresponding to 3 versions of the focal spot size; lines can be fitted by scaling $\mathcal{E}_{\max} \propto \mathcal{E}_{\rm L}^{0.8}$ up to $\mathcal{E}_{\max} \lesssim 200$ MeV and by $\mathcal{E}_{\max} \propto \mathcal{E}_{\rm L}$ for higher energy gains when a transition begins to the RPD regime.

Figure 4 shows a correlation of the proton maximum energy with the laser power $\mathcal{P}$ for $n_e = 100 n_{\rm cr}$, where points correspond to a thickness l close to optimal, i.e., $n_e l \approx \sigma_{\rm opt}$. Narrowing the set of points by the additional constraint that the laser pulse length is of the order of the focal spot size $L_p \sim D$, we obtain a strip aligned along the dependence $\mathcal{E}_{\max} \propto \mathcal{P}^{1/2}$. Once again, we see a degeneration of a complex dependence of the ion maximum energy from many parameters to a dependence from a fewer number of parameters. This is a manifestation of the regime of ion acceleration described in Refs. [1,13]. The square-root dependence of the ion maximum energy on the laser power is consistent with the prediction made in Ref. [13]. Following these references, one can represent the irradiated spot as an uniformly charged oblate ellipsoid with size $l \times D \times D$, $l < D$, and charge density $+\eta e n_e$, where η is a portion of electrons swept away by the laser pulse. Assuming that the target electron areal density is optimal, $n_e l = 0.4 a n_{\rm cr} \lambda$, one can obtain the maximum energy of the ion with charge Ze accelerated by the electric field of the ellipsoid (for $l \ll D$): $\mathcal{E}_{\max} \approx \eta Z (\mathcal{P}[{\rm PW}])^{1/2} \times 228$ MeV, where $\mathcal{P}$ is the laser peak power. The condition that the optimal laser pulse length should be greater than or of the order of the focal spot size, $L_p \gtrsim D$, turns out to be necessary to prevent return currents from affecting the ion acceleration (both the current formed by returning electrons and that produced by electrons from a surrounding less irradiated and relatively cold plasma).

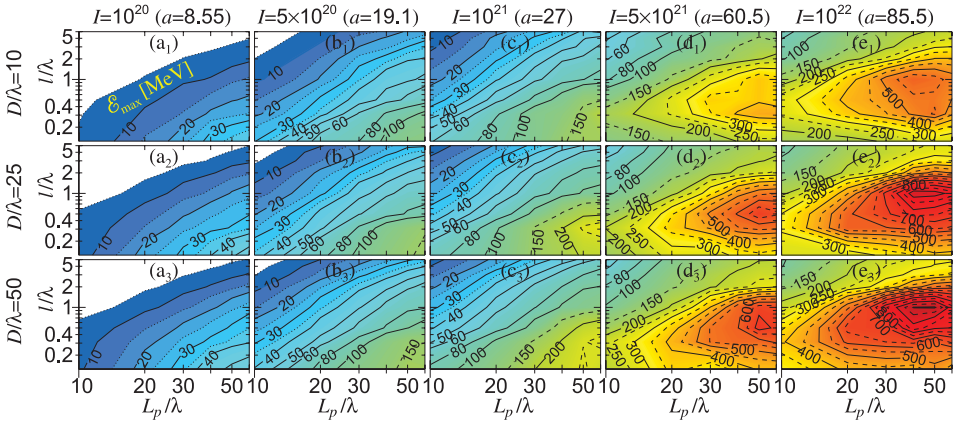

FIG. 2 (color). Proton maximum energy (contours) vs laser length and target thickness (log-log scale) for different laser intensities [columns (a)–(e)] and different laser focal spots (rows 1–3), for $n_e = 100 n_{\rm cr}$.

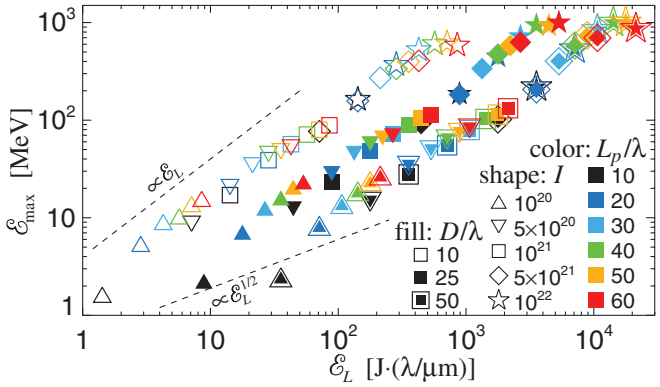

FIG. 3 (color). Proton maximum energy vs laser pulse energy for $l = \lambda$, $n_e = 100n_{cr}$. The dashed lines exemplify possible scalings.

In conclusion, our multiparametric simulations show that, in the process of ion acceleration by an intense laser pulse from a double layer target, at given laser intensity I, the dependence of the ion maximum energy from the target thickness l and density n_e is reduced to a dependence on the electron areal density $\sigma = n_e l$. At a given intensity, the highest ion energy gain occurs at the optimal electron areal density of the target σ_{opt}, which is approximately proportional to the square root of intensity $\sigma_{opt} \propto I^{1/2}$. If the target electron areal density is less than the optimal value, the laser pulse is more transmitted rather than absorbed; if it is greater, the laser pulse reflection increases, making the interaction less efficient for ion acceleration. In the case of thin targets and optimal laser pulse duration, the ion maximum energy scales as the square root of the laser pulse power. With this scaling, the laser-driven ion acceleration up to 200–300 MeV, which is necessary for hadron therapy, can be obtained with a petawatt laser with subpicosecond duration. At increasing intensity, we see a transition to the RPD regime, where the ion maximum energy becomes proportional to the laser pulse energy.

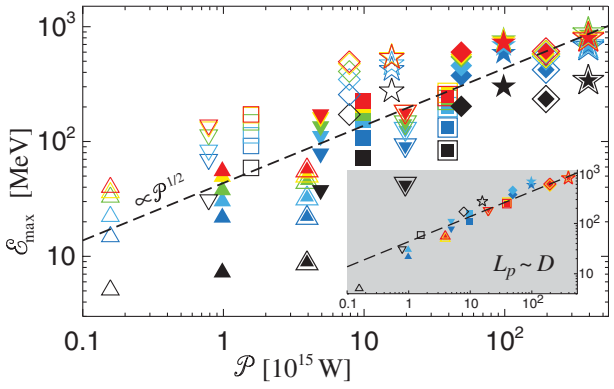

FIG. 4 (color). Proton maximum energy vs laser power for optimal plasma slab thickness and $n_e = 100n_{cr}$. The inset is for $L_p \sim D$.

We thank Professor S. V. Bulanov for the formulation of the problem and helpful suggestions. We thank Professor H. Daido, Professor C. Ma, Professor G. Mourou, Professor K. Nemoto, and Professor A. Noda for discussions, MEXT and JST CREST for support.

*Also at Moscow Institute of Physics and Technology, Dolgoprudnyi, 141700 Russia.

[1] S. V. Bulanov and V. S. Khoroshkov, Plasma Phys. Rep. **28**, 453 (2002); S. V. Bulanov *et al.*, *ibid.* **28**, 975 (2002); S. V. Bulanov *et al.*, Phys. Lett. A **299**, 240 (2002); T. Zh. Esirkepov *et al.*, Phys. Rev. Lett. **89**, 175003 (2002).

[2] M. Roth *et al.*, Phys. Rev. Lett. **86**, 436 (2001); V. Yu. Bychenkov *et al.*, Plasma Phys. Rep. **27**, 1017 (2001); S. Atzeni *et al.*, Nucl. Fusion **42**, L1 (2002).

[3] I. Spencer *et al.*, Nucl. Instrum. Methods Phys. Res., Sect. B **183**, 449 (2001).

[4] K. W. D. Ledingham *et al.*, J. Phys. D **36**, L79 (2003).

[5] T. Esirkepov *et al.*, Phys. Rev. Lett. **92**, 175003 (2004); S. V. Bulanov *et al.*, Plasma Phys. Rep. **30**, 196 (2004).

[6] S. V. Bulanov *et al.*, Nucl. Instrum. Methods Phys. Res., Sect. A **540**, 25 (2005).

[7] G. A. Mourou *et al.*, Phys. Today **51**, No. 1, 22 (1998); S.-W. Bahk *et al.*, Opt. Lett. **29**, 2837 (2004); I. N. Ross *et al.*, Opt. Commun. **144**, 125 (1997); T. Tajima and G. Mourou, Phys. Rev. ST Accel. Beams **5**, 031301 (2002).

[8] S. P. Hatchett *et al.*, Phys. Plasmas **7**, 2076 (2000).

[9] M. Borghesi *et al.*, Phys. Plasmas **9**, 2214 (2002); M. Borghesi *et al.*, Phys. Rev. Lett. **92**, 055003 (2004).

[10] T. E. Cowan *et al.*, Phys. Rev. Lett. **92**, 204801 (2004).

[11] A. Maksimchuk *et al.*, Phys. Rev. Lett. **84**, 4108 (2000); A. J. Mackinnon *et al.*, *ibid.* **88**, 215006 (2002).

[12] A. V. Gurevich *et al.*, Sov. Phys. JETP **22**, 449 (1966); S. C. Wilks *et al.*, Phys. Plasmas **8**, 542 (2001); P. Mora, Phys. Rev. Lett. **90**, 185002 (2003); S. V. Bulanov *et al.*, Plasma Phys. Rep. **30**, 18 (2004).

[13] S. V. Bulanov *et al.*, in *The Physics of Ionized Gases: 22nd Summer School and International Symposium on the Physics of Ionized Gases*, edited by L. Hadžievski, T. Grozdanov, and N. Bibic, AIP Conf. Proc. No. 740 (AIP, New York, 2004), p. 414.

[14] K. Nemoto *et al.*, Appl. Phys. Lett. **78**, 595 (2001); A. J. Mackinnon *et al.*, Phys. Rev. Lett. **86**, 1769 (2001); Y. Sentoku *et al.*, Appl. Phys. B **74**, 207 (2002).

[15] K. Matsukado *et al.*, Phys. Rev. Lett. **91**, 215001 (2003).

[16] T. Zh. Esirkepov, Comput. Phys. Commun. **135**, 144 (2001).

[17] A. V. Kuznetsov *et al.*, Plasma Phys. Rep. **27**, 211 (2001).

[18] V. A. Vshivkov *et al.*, Phys. Plasmas **5**, 2727 (1998); S. V. Bulanov *et al.*, in *Reviews of Plasma Physics*, edited by V. D. Shafranov (Kluwer Academic, New York, 2001), Vol. 22, p. 227.

[19] T. Zh. Esirkepov *et al.*, JETP Lett. **70**, 82 (1999); S. V. Bulanov *et al.*, *ibid.* **71**, 407 (2000); Y. Sentoku *et al.*, Phys. Rev. E **62**, 7271 (2000); H. Ruhl *et al.*, Plasma Phys. Rep. **27**, 363 (2001).